Catal Lett (2008) 121:324–330
DOI 10.1007/s10562-007-9342-z

Preparation and Characterization of a Magnetic Solid Acid for Esterification of Ammonium Lactate with n-Butanol

Qunhui Wang · Wenchao Zhao · Xiaohong Sun · Wenjun Zhao

Received: 21 September 2007 / Accepted: 5 November 2007 / Published online: 21 November 2007

Abstract One kind of magnetic solid acid (MSA) was prepared by thermolysis of nickel sulfate with ferric hydroxide at 1,123 K. Its properties, such as magnetism and surface acidity, were investigated by PPMS, FTIR-NH_3, TPD-NH_3, XRF, XRD techniques. Its saturation magnetization is estimated to be 10.72 emu/g and a hysteretic feature with a remnant magnetization (2.76 emu/g) and coercivity (0.15 kOe) at 300 K is exhibited. The results also reveal that MSA solely possesses mild Lewis acid sites and four crystalline phases. Its catalytic activity for esterification of ammonium lactate with n-butanol was tested. The esterification yield (Ey) will be significantly enhanced when $SnCl_2 \cdot 2H_2O$ is added. The highest Ey will be up to 87.3% when the complex concentration is 5 wt% (mass ratio of $SnCl_2 \cdot 2H_2O$ to MSA = 4:1). The possible reasons correlating with the esterification performance of the complex system are discussed.

Q. Wang (✉) · W. Zhao
Department of Environmental Science and Technology, Harbin Institute of Technology, Harbin 150090, People's Republic of China
e-mail: wangqh59@sina.com

Q. Wang
Department of Environmental Engineering, University of Science and Technology Beijing, Beijing 100083, People's Republic of China

W. Zhao
Nano-organic Photoelectronic Laboratory, Technical Institute of Physics and Chemistry, Chinese Academy of Sciences, Beijing 100080, People's Republic of China

X. Sun
Beijing Agro-Biotechnology Research Center, Beijing 100097, China

Keywords Esterification · Ammonium lactate · Catalysis · Magnetic solid acid

1 Introduction

Lactate esters are nonvolatile, nontoxic and degradable compounds, which are increasingly used in foods, cosmetics and pharmaceutical formulations due to their hygroscopic, emulsifying and exfoliating properties. They can be anticipated to replace a range of environmental-damaging or toxic solvents [1–5].

Conventionally, lactate esters are synthesized by esterification of lactic acid with corresponding alcohols [6–9]. Lactic acid can be produced by either chemical synthesis or lactic acid fermentation of carbohydrate [10]. In the latter process, lactate (such as ammonium lactate) instead of lactic acid will be produced. Before the esterification process, complex separation steps are needed to recover and purify the product from the crude fermentation broth [11], resulting in large amounts of by-product. Furthermore, because of the acidity of lactic acid, an acid resistance reactor has to be employed in the esterification process. So the mass production in this approach is technically and economically uncompetitive [4]. Whereas ammonium lactate appears to offer some important advantages as a raw material for lactate ester preparations, the substitution of fermentation broth for ammonium lactate as the primary lactic acid fermentation product would be more competitive [12].

Esterification is one kind of acid-promoted reaction, and for acid-promoted reactions, the catalysis of solid acid is a very rewarding research field [13–17]. The solid acid catalysts, including sulfated metal oxides [18–20], are considered as the candidates of potential substitution for liquid acid catalysts due to their characteristics, such as

non-toxicity, non-corrosiveness, less expensive and are easy to recover and reuse [21–25]. The possibility to modify their acid properties in a predetermined direction through a synthesis treatment and a post-synthesis treatment is another feature.

Yet their recovery would be tremendously influenced by the negative impact of impurities contained in the fermentation broth, while they were utilized for esterification with fermentation broth as the starting materials. In this regard, magnetic solid acid (MSA) would be an alternative, for its magnetic properties could broaden the scope of its recovery methods. During the conventional preparation of MSA based on sulfated metal oxides, the magnetic core was prepared firstly, which would behave as the supporter, and then a shell modified by sulfate ion was covered on the supporter surface [24–27]. The process for magnetization formation and that for acidity formation were separated.

In the present study, a simplified approach to prepare MSA was explored. Furthermore, the catalytic activity of the complex of MSA and $SnCl_2 \cdot 2H_2O$ for esterification of ammonium lactate with n-butanol was studied, and the possibility of lactic acid fermentation broth as the starting material for synthesis of lactate esters was analyzed too.

2 Experimental Methods

2.1 Catalyst Preparation

All reagents were of reagent-grade purity and were used without further purification.

The MSA was prepared as follows. Firstly, the precipitate of ferric hydroxide was obtained by adding aqueous ammonia (25%) slowly into an aqueous solution of ferric sulfate at room temperature under vigorously mechanical stirring until pH of the mother liquid reached about 7. The precipitate slurry, obtained in this way, was centrifuged and the solvent was decanted to collect a red-brown solid. The red-brown solid collected was dried at 373 K for 20 h.

The dried precipitate was powdered below 100 meshes, and then it was impregnated with a desired aqueous solution of $NiSO_4 \cdot 6H_2O$, followed by evaporating the water, drying and calcining in air at 1,123 K for 3 h. It was used as a catalyst after evacuation at 1,123 K for 1 h. The catalyst was denoted as MSA.

The MSA was stored in a desiccator to prevent it from absorbing moisture.

2.2 Sample Characterization

The fresh samples were divided into several portions where different portions were used for different analyses to avoid the correlations between the treatments in different analysis methods.

2.3 X-ray Fluorescence and X-ray Diffraction

The XRF measurements were performed on an Axios pw4400 XRF wavelength dispersive spectrometer with an Rh X-ray tube target.

The X-ray diffraction data of the sample powder were collected using a Rigaku D/max-RB instrument with Cu Kα radiation of 50 kV $\times$ 40 mA and a graphite monochromator.

2.4 Magnetic Properties Analysis

Magnetization measurements were carried out using the physical property measurement systems (PPMS) of a quantum design.

2.5 Infrared Spectroscopy with Adsorbed Ammonia, NH_3-FTIR

The MSA sample was compressed into a self-supporting wafer of 10 mg/cm^2 thickness and placed in a heatable sample-holder between CaF_2 windows of a metal IR cell. The wafer was treated with flowing oxygen at 573 K for 2 h under a vacuum, namely residual pressure $<10^{-2}$ Pa, after the cell was evacuated for 30 min. The wafer was then cooled to room temperature and contacted with ammonia at 270 Pa for 30 min, and then the cell containing the ammonia was closed. The cell was transferred into the IR spectrometer to record the spectrum, whilst still under vacuum (residual pressure $<10^{-2}$ Pa).

Before dosing appropriate amounts of ammonia, the spectrum of the sample under vacuum and the background spectrum without the sample in place were recorded. The spectra were collected using a Nicolet AVATAR 360 FTIR ESP spectrometer, and 256 scans were averaged at a nominal resolution of 4 cm^{-1}. A curve-fitting computer program was used to resolve the overlapping peaks.

2.6 Temperature Programmed Desorption of Ammonia, NH_3-TPD

NH_3-TPD was performed with an AutoChem 2910 analyzer. The NH_3-TPD measurements were carried out using a conventional flow-through reactor, which was attached to a vacuum system to evacuate the reactor and contact the sample with ammonia gas. The sample (about 200 mg) was

activated. After pouring He (30 mL/min) at 873 K for 0.5 h, the reactor was then evacuated for 0.5 h, and the resulting sample was cooled to 373 K, that is to say, the adsorption temperature. The NH_3 adsorption was performed by introducing 60–100 μl of NH_3 in helium gas flow (20 mL/min) for 30 min. The dried helium flow was continued for an additional 30 min to allow removal of any physisorbed adsorbent. Desorption was conducted under the same helium flow, while the reactor temperature was ramped up to 873 K at a rate of 10 K per min. The rate of ammonia desorption during the programmed temperature rise was detected using a thermal conductivity detector (TCD), and the detector signal was recorded as the TPD profile of ammonia for the samples.

2.7 Esterification Studies

The apparatus for esterification and rectification is schematically showed in Fig. 1. A 500 mL three-necked flask was equipped with a rectifying column filled with ceramic rings, a thermometer and a polytetrafluoroethylene stirrer. The rectifying column with a 300 mm length and a diameter of 40 mm was connected with a water condenser and a water separator where water was added before reaction and the water level approached a control valve 8.

The reagent ammonium lactate was obtained as follows. Aqueous ammonia (25%) was added into lactic acid (85%) with stirring until pH was up to 7. After that, fresh ammonium lactate, fresh n-butanol and the catalyst would be added into the reactor with a certain molar ratio. When the temperature of the reactor reached over 373 K, the azeotropic mixture containing n-butanol and water would be formed. Owing to low solubility of butanol in water, the condensed overhead phase separated into a light butanol phase and a heavy water phase, and only the light butanol phase was returned through the control valve 8 to the rectifying column, another heavy water phase was removed through the sampling valve 7. Ammonia generated in the esterification procedure was vented through a vent-pipe 11, and then absorbed by distilled water for recycle.

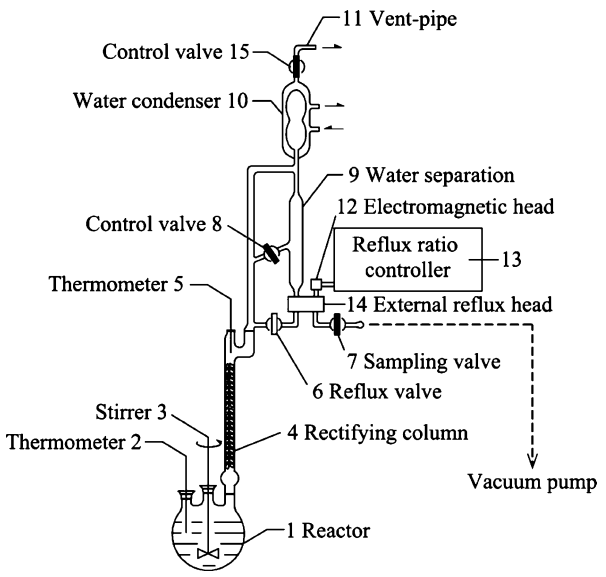

Fig. 1 The schematic diagram of apparatus for esterification and rectification

After a desired reaction time at desired reaction temperature, the reaction liquid obtained in the esterification procedure was subjected to rectification by closing control valve 8 and 15. The rectifying process was comprised of two sections. Firstly, the unreacted butanol was recovered by reducing the pressure to 20,000 Pa, controlling a reflux ratio 1:1 with a reflux ratio control system and keeping a temperature 353 K at a column top. Next, on the conditions of temperature 345 K at a column top and a reflux ratio 1:1, a pressure was continuously reduced to 2,000 Pa to obtain the ultimate product (n-butyl lactate). The reflux ratio control system consists of an external reflux head, a reflux ration controller and control power. The purity of the ester was characterized by gas chromatography.

In order to represent the esterification yield, a new symbol Ey was used. It was estimated according to the following formula:

$$\mathrm{Ey} = \frac{\text{Actual yield of butyl lactate} \times \text{Purity}}{\text{Theoretical yield of butyl lactate}} \times 100\%$$

where purity refers to the percentage of n-butyl lactate in the ultimate product.

3 Results and Discussion

3.1 Elements and Crystal Structure of MSA

The content of elements in MSA was analyzed by XRF, which was shown in Table 1. According to it, the main elements except O in MSA were Ni, Fe and S. The existence of S element would be due to the acidity of the MSA, while the elements of Ni and Fe would contribute to the magnetic properties.

The crystal phase was identified by XRD, which was shown in Fig. 2. In the diffraction pattern, the diffraction

Table 1 Quantitative analysis of elements in MSA by XRF

Element	Content (mass %)
Ni	29.41
Fe	37.64
S	3.17

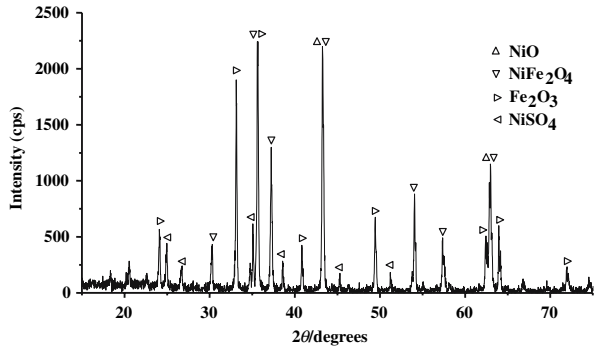

Fig. 2 X-Ray diffraction pattern of MSA

lines in agreement with those of NiO, $NiFe_2O_4$, Fe_2O_3 and $NiSO_4$ were found. They should be originated from the thermolysis and interaction between $Fe(OH)_3$ and $NiSO_4$. The decomposition of $Fe(OH)_3$ would form Fe_2O_3, which could react with $NiSO_4$ to synthesize $NiFe_2O_4$. The existence of S element detected by XRF would be mainly owing to the decomposition of $NiSO_4$, though the temperature for MSA preparation had been over the decomposition temperature of $NiSO_4$ (1,113 K) [30].

3.2 Magnetic Properties

The sample indicated a remnant magnetization and coercivity, which exhibited a hysteretic feature. Figure 3 presents the magnetization of the sample at 300 K. The remnant magnetization and coercivity for the sample at 300 K are 2.76 emu/g and 0.15 kOe, respectively. Extrapolating the magnetization versus the inverse of the field curve to $1/H = 0$, the saturation magnetization is estimated to be 10.72 emu/g.

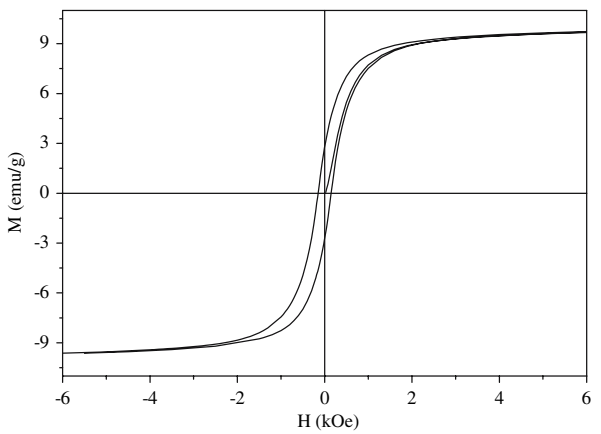

Fig. 3 Variation of magnetization with the applied field at 300 K

3.3 Surface Acidic Properties

3.3.1 NH_3-FTIR

Infrared spectra of MSA are shown in Fig. 4. In the spectrum (a), four obvious bands were found at 1,218, 1,161, 1,040, and 985 cm^{-1}. These bands lied in the SO stretching frequency region, and the former two and the latter two bands were assigned to the asymmetric and symmetric stretching frequencies of the O=S=O and O–S–O groups, respectively.

The spectrum with the four bands is similar to that of the inorganic chelating bi-dentate complexes mentioned by several authors [31, 32]. Most of the S=O bonds in MSA would possess partial double-bond character, and the electron pair is partially located around O and S atoms.

In the spectrum (a), faint absorption bands at 1,395 and 920 cm^{-1} may be assigned to the stretching vibrations of organic sulfate compounds on the surface of MSA, like the covalent double SO bonds in organic sulfates. However, compared to the absorption intensity in the range of 1,200–900 cm^{-1}, the organic sulfate compounds were pretty little, which could not be found in XRD profile. In FTIR spectrum, the coexistence of organic sulfate compounds and chelating bi-dentate complexes would slightly account for the broad bands in the SO stretching frequency region yet.

In the 1,450–1,800 cm^{-1} region of the spectrum (b), a band at 1,625 cm^{-1} indicates the presence of coordinated ammonia, and no band at 1,430 cm^{-1} indicates the absence of ammonia ion, when ammonia was adsorbed on the MSA sample. This reveals that the catalyst solely possesses Lewis acidity, that no Brønsted acidity is found, and that the cation ions in the bi-dentate complexes would act as Lewis acid sites. In the XRD profile, nickel sulfate has

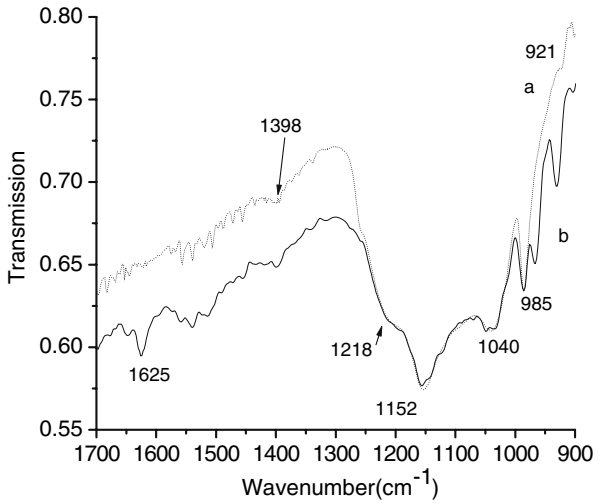

Fig. 4 Infrared spectra of MSA. (**a**: no NH_3 adsorption; **b**: with NH_3 adsorption)

been indicated, so that the band at 1,625 cm^{-1} would be attributed to a nickel ion.

From the comparison of the asymmetric stretching frequencies of double SO bonds in the spectrum (a) with that in spectrum (b), no shift was found for the inorganic sulfate compounds, and a small shift was found for the organic sulfate compounds. Such a result suggests that a small change of the electronic structure in the surface sulfur complex takes place by the adsorption of ammonia molecules.

3.3.2 NH_3-TPD

The TPD profile of ammonia on MSA is shown in Fig. 5. The ammonia desorption was observed over a wide temperature range for the sample. Only one main peak was found yet at 473 K. From the FTIR spectra, it is reasonable to assign the ammonia species desorbed at 473 K to coordinated NH_3 at Lewis acid sites. The absence of the adsorption peak at high temperature also suggests that the acidic strength of the sample was not strong and that it was in accord with the result of the shift mentioned in NH_3-FTIR spectra. The main reason would be the formation of the sulfur complex with a covalent SO double bond limited, while such compounds would promote the generation of acidity.

3.4 Catalytic Activities for Esterification

In this study, we mainly investigated two catalytic systems. One was single MSA system, and the other was the complex of MSA and $SnCl_2 \cdot 2H_2O$.

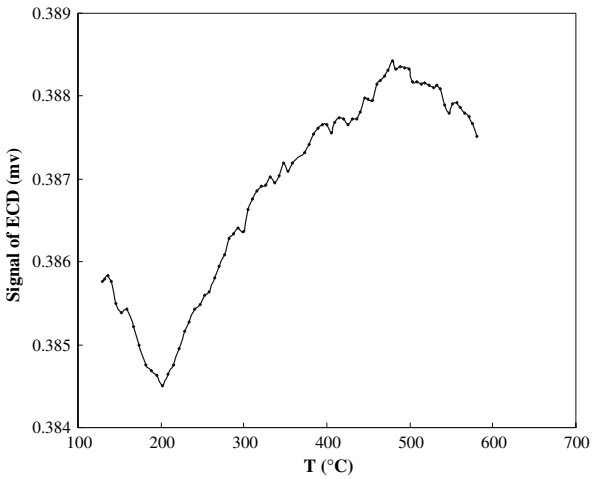

Fig. 5 TPD profile of ammonia on MSA

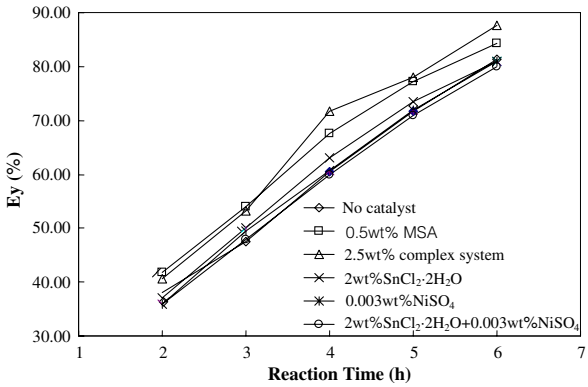

Fig. 6 Esterification yield as a function of reaction time against different catalytic systems. (The mass ratio of $SnCl_2 \cdot 2H_2O$ to MSA in the complex system was 4:1. The reaction temperature was 400 K)

The changes of the esterification yield as a function of reaction time against different catalytic systems were shown in Fig. 6. By inspection of the data, it is apparent that the background activity is significant. Ey could be up to 81.4% in 6 h without catalyst added. The activity of $SnCl_2 \cdot 2H_2O$ was not obvious enough to be compared with MSA, which possesses significant activity in excess of the background. When the complexes of $SnCl_2$ and MSA were used as catalysts, the most significant activity for esterification was observed yet. Meanwhile, the catalytic systems of $NiSO_4$ and $NiSO_4/SnCl_2 \cdot 2H_2O$ were also examined to testify the effective components in MSA during the esterification, but the catalytic activity was not found, respectively.

Figure 7 shows the effect of mass ratio of $SnCl_2 \cdot 2H_2O$ to MSA on the esterification yield with a constant MSA concentration. The esterification yield would increase with the addition of mass ratio of $SnCl_2 \cdot 2H_2O$ to MSA before

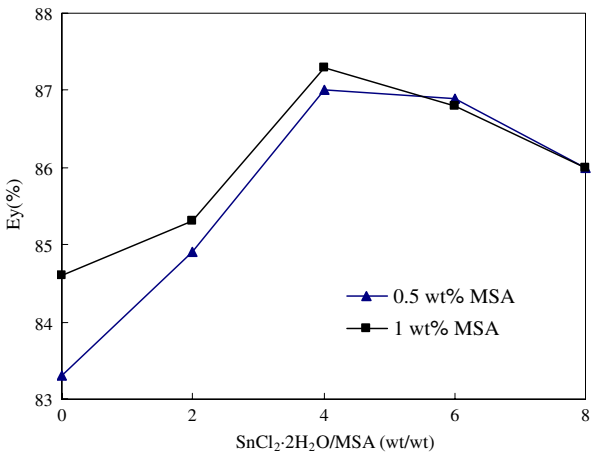

Fig. 7 Effect of mass ratio of $SnCl_2 \cdot 2H_2O$ to MSA on esterification yield with a constant MSA concentration. (The reaction time was 6 h. The reaction temperature was 400 K)

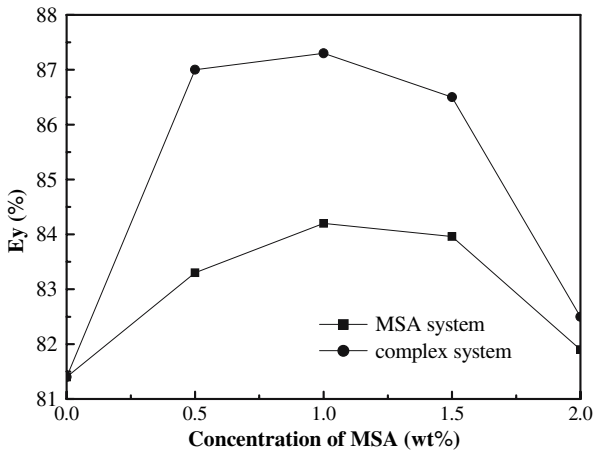

Fig. 8 Effect of MSA concentration on esterification yield at two different systems. (For the complex system, the mass ratio of $SnCl_2 \cdot 2H_2O$ to MSA was 4:1. The reaction time was 6 h, and the reaction temperature was 400 K)

the mass ratio of $SnCl_2 \cdot 2H_2O$/MSA was up to 4:1, which would cause a maximum of esterification yield. However, over the point, the increase of $SnCl_2 \cdot 2H_2O$/MSA would not make significant effect to increase the esterification yield.

Figure 8 illustrates the effect of the catalytic concentration (relative to a reagent of ammonium lactate) on the esterification yield with two different catalytic systems. The results indicate that the yields of n-butyl lactate in both catalytic systems would increase with increasing the concentration of the catalyst, respectively, and a maximum yield would be observed, when the catalytic concentration was up to some value. When the concentration exceeds the point, the catalytic activities of the tow complexes decline. For MSA, the maximum Ey was 84.2%, when its concentration was 1 wt%. As for the complex of MSA and $SnCl_2 \cdot 2H_2O$, when the complex concentration was 5 wt% with the mass ratio of MSA/$SnCl_2 \cdot 2H_2O$ of 1:4, the yield of n-butyl lactate would reach its maximum of 87.3%. The appearance of the maximal Ey in each catalytic system could be attributed to the side effects by an excess addition.

For the esterification of ammonium lactate with n-butanol, the reaction process consists of two steps. The first step is the conversion from ammonium lactate to lactic acid, which results in the release of ammonia, and the second step was the esterification of lactic acid with n-butanol [12]. $SnCl_2 \cdot 2H_2O$ would behave as Lewis acid with undergoing the self-condensation to form activated hydrate, which would be responsible for the catalytic activity [32, 33]. For the esterification of lactic acid, the complex system could show a significant catalytic activity, and then the esterification yield could be up to 79.8% within 3 h (Data not showed). For the esterification of ammonium lactate, the complex was not active (see Fig. 6). The main reason may be its poor activity for the first step of esterification.

From the NH_3-FTIR spectrum of the MSA catalyst, it is known that on the surface of the catalyst, only Lewis typed acid sites were found. Furthermore, the results from NH_3-TPD curve and NH_3-FTIR spectra indicate that the acid strength is not strong. It seemed that the MSA systems would not be effective for the esterification. The data has yet testified the catalytic acitivity of MSA for the esterification from Figs. 6 and 8. We could find that $NiSO_4$ and $NiSO_4/SnCl_2 \cdot 2H_2O$ nearly have no catalytic activity compared with MSA and MSA/$SnCl_2 \cdot 2H_2O$ from Fig. 6, though $NiSO_4$ was the main compounds containing an S element in MSA. One probable reason may be that the origin of the acidity was mainly organic sulfate compounds, which could form the Lewis acid sites with relatively strong strength. Such Lewis acid sites could convert to Brønsted acid sites if it adsorbed water. For the first step, Brønsted acid is prone to be more effective than Lewis acid. As a result, the esterification in the fist step is likely to be especially enhanced by the MSA catalyst, and then Ey was increased. When the catalyst having vacant sites in some degree [34] with activation could exist, some side reactions would be induced, which caused the decline of n-butyl lactate yield.

For the complex system of MSA and $SnCl_2 \cdot 2H_2O$, there maybe exist a new-formed coordination structure between MSA and the tin(II)-oxide cluster, which would strengthen the acid strength for the electronic induction effect. At the same time, in the vacant sites with activation, the excess coordination sites on the surface of MSA could be occupied and reduced especially. In this case, the esterification would be not only strengthened for the increase of acid strength, but also the side reaction could be reduced. So the complex system shows the most significant activity for the esterification.

Furthermore, the coordination process in the complex system could be influenced by some factors, such as distribution of acid sites with different acidic strength, and the obstacles from the thin pore channel in the catalyst for the pervasion of Sn to coordinate with acidic centers in MSA. So there exists an optimal mass ratio of the two components, as well as a maximum esterification yield.

4 Conclusions

The method of preparing the MSA by the thermolysis and the interaction of nickel sulfate with ferric hydroxide at a certain temperature was feasible, and then the formation of magnetic properties and acidity could be achieved in one process.

For MSA prepared at 1,123 K, the saturation magnetization, the remnant magnetization and the coercivity are estimated to be 10.72, 2.76 emu/g and 0.15 kOe at 300 K, respectively. However, the acidity of the resultant magnetic material was not strong, and it would only possess the Lewis acid sites.

For the esterification of ammonium lactate with n-butanol, the complex of MSA and $SnCl_2 \cdot 2H_2O$ was an effective catalyst, though MSA could slightly catalyze the reaction. The addition of $SnCl_2 \cdot 2H_2O$ could heighten Ey yet. The highest Ey could be up to 87.3%, when the complex concentration was 5 wt% with the mass ratio of $SnCl_2 \cdot 2H_2O$/MSA equaling to 4:1.

The significant catalytic activity of the complex of MSA and $SnCl_2 \cdot 2H_2O$ for the esterification of ammonium lactate with n-butanol also indicates the possible usage in the esterification of fermentation broth with ammonium lactate as the primary fermentation product.

Acknowledgment This work was financially supported by National Science Foundation of China (50278024) and the Scientific Research Foundation for the Returned Overseas Chinese Scholars, Heilongjiang Province (LC02C03).

References

1. Clary JJ, Feron VJ, van Velthuijsen JA (1998) Regul Toxicol Pharm 27:88
2. Bowmer CT, Hooftman RN, Hanstveit AO, Venderbosch PWM, van der Hoeven N (1998) Chemosphere 37:1317
3. Pirozzi D, Greco G Jr (2004) Enzyme Microb Technol 34:94
4. Datta R, Tsai SP, Bonsignore P, Moon SH, Frank JR (1995) FEMS Microbiol Rev 16:221
5. Nikles SM, Piao M, Lane AM, Nikles DE (2001) Green Chem 3:109
6. From M, Adlercreutz P, Mattiasson B (1997) Biotechnol Lett 19:315
7. Torres C, Otero C (1999) Enzyme Microb Technol 25:745
8. Yadav GD, Kulkarni HB (2000) React Funct Polym 44:153
9. Choi JI, Hong WH, Chang HN (1996) Int J Chem Kinet 28:37
10. Milcent S, Carrere H (2001) Sep Purif Technol 22–23:393
11. Kertes AS, King CJ (1986) Biotechnol Bioeng 28:269
12. Filachione EM, Costello J (1952) Ind Eng Chem 44:2189
13. Storck S, Maier WF, Miranda Salvado IM, Ferreira JMF, Guhl D, Souverijns W, Martens JA (1997) J Catal 172:414
14. Bhatt N, Patel A (2005) J Mol Catal A 238:223
15. Bhagiyalakshmi M, Shanmugapriya K, Palanichamy M, Arabindoo B, Murugesan V (2004) Appl Catal A Gen 267:77
16. Sejidov FT, Mansoori Y, Goodarzi N (2005) J Mol Catal A 240:186
17. Kuriakose G, Nagaraju N (2004) J Mol Catal A 223:155
18. Shanmugam S, Viswanathan B, Varadarajan TK (2004) J Mol Catal A 223:145
19. Furuta S, Matsuhashi H, Arata K (2004) Appl Catal A Gen 269:187
20. El-Sharkawy EA, Al-Shihry SS (2004) Mater Lett 55:2122
21. Reddy BM, Sreekanth PM, Reddy VR (2004) J Mol Catal A 225:71
22. Corma A (1995) Chem Rev 95:559
23. Corma A, Garcia H (2003) Chem Rev 103:4307
24. Okuhara T (2002) Chem Rev 102:3641
25. Harmer MA, Sun Q (2001) Appl Catal A Gen 221:45
26. Zhang ML, Wang J, Mei CS, Jing XY, Duan X (2002) Chem J Chin Univ 23:1347
27. Chang Z, Li F, Duan X, Zhang ML (2001) Chin. J Inorg Chem 17:366
28. Chang Z, Guo CX, Duan X, Zhang ML (2003) Chin J Catal 24:47
29. Ramankutty CG, Sugunan S (2001) Appl Catal A Gen 218:39
30. Dean JA (1999) Lange's handbook of chemistry. McGraw-Hill, New York
31. Yamaguchi T, Jin T, Tanabe K (1986) J Phys Chem 90:3148
32. Jin T, Machida M, Yamaguchi T, Tanabe K (1984) Inorg Chem 23:4396
33. Moon SI, Lee CW, Miyamoto M, Kimura Y (2000) J Polym Sci Pol Chem 38:1673
34. Kim KW, Woo SI (2002) J Macromol Sci-Rev Macromol Chem Phys 203:2245